PERGAMON

Engineering Fracture Mechanics 62 (1999) 339–350

Engineering Fracture Mechanics

Thermal shock cracking in a metal-particle-reinforced ceramic matrix composite

Z-H. Jin, R.C. Batra*

Department of Engineering Science and Mechanics, MC-0219, Virginia Polytechnic Institute and State University, Blacksburg, VA 24061, USA

Received 30 June 1998; received in revised form 30 November 1998

Abstract

We study thermal crack shielding and thermal shock damage in a double-edge cracked metal-particle-reinforced ceramic matrix composite subjected to sudden cooling at the cracked surfaces. Under severe thermal shocks, the crack will grow but will be bridged by the plastically stretched metal particles. A linear softening bridging law is used to describe the metal particle bridging behavior. An integral equation of the thermal crack problem incorporating the bridging effect is derived and the thermal stress intensity factor at the bridged crack tip is calculated numerically. It is found that the thermal stress intensity factor is significantly reduced by the metal particle bridging. While the crack growth in thermally shocked monolithic ceramics is unstable, the composite can withstand sufficiently severe thermal shocks without failure.

Keywords: Thermal stress; Thermal fracture; Stress intensity factor; Crack bridging

1. Introduction

Metal-particle-reinforced ceramic matrix composites (MPCMCs) are promising candidates for future high temperature applications. MPCMCs have superior crack growth resistance when compared with monolithic ceramics and possess excellent high temperature strength properties when compared with metal alloys. Significant progress has been made in understanding the crack growth resistance and strength behavior of MPCMCs and other ductile phase reinforced brittle systems subjected to mechanical loads, for example, see Refs.

* Corresponding author. Tel.: +1-540-231-6051; fax: +1-540-231-4574.
E-mail address: rbatra@vt.edu (R.C. Batra)

PII: S0013-7944(98)00112-X

[1–9]. However, little effort has been devoted to understanding thermal shock fracture behavior of MPCMCs. The knowledge of thermal cracking and damage in MPCMCs is important for the design of such components as engines and turbines which are frequently subjected to thermal shocks. It is expected that thermal cracking and damage resistance of MPCMCs will be enhanced over that of monolithic ceramics.

The basic toughening mechanism in MPCMCs is metal particle bridging [1–5,8,9]. When a crack grows in the brittle matrix, the metal particles at the crack surface will deform plastically and bridge the crack surfaces thereby reducing the stress intensity at the crack tip. The effective fracture toughness and the residual strength are thus enhanced. The aim of the present study is to investigate thermal cracking and damage behavior of MPCMCs. We consider a double-edge cracked MPCMC strip subjected to sudden cooling at the cracked surfaces. Thermal stress intensity factors are calculated for both monolithic ceramics and MPCMCs and the thermal crack shielding effect of the metal particle bridging is discussed. Crack growth length in the specimen due to a given thermal shock is also investigated.

2. Thermal crack shielding

2.1. Temperature field

Consider an infinite MPCMC strip of width $2b$ with double-edge cracks of length a as shown in Fig. 1. The strip is initially at a constant temperature T_0 and its surfaces $x_1 = \pm b$ are

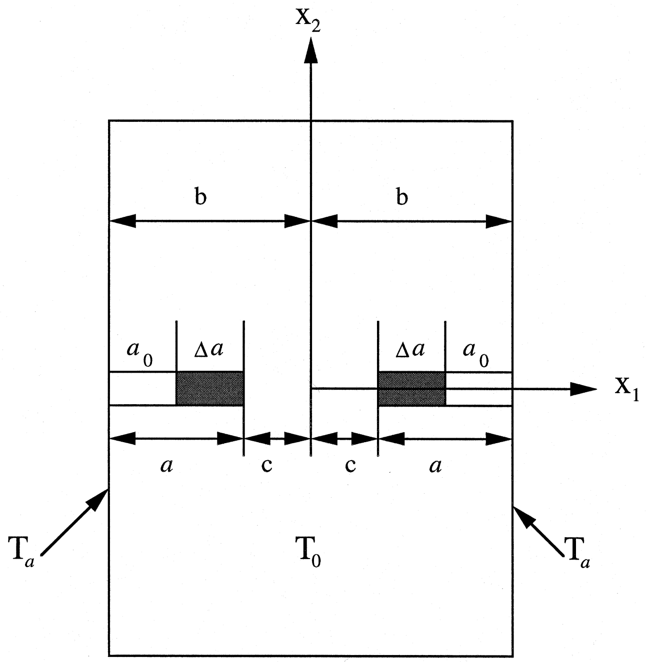

Fig. 1. A double-edge cracked strip subjected to a thermal shock.

suddenly cooled to a temperature $T_a (T_a < T_0)$. This thermal shock problem may be used to study the thermal stresses in a quenched specimen. Since the heat will flow only in the x_1-direction, the initial and boundary conditions for the temperature field are

$$T(x_1,0) = T_0 \tag{1}$$

$$T(x_1,t) = T_a, \quad x_1 = \pm b, \quad t > 0 \tag{2}$$

We regard the MPCMC as an isotropic material. The temperature field in the strip can be expressed as [10]

$$\frac{T - T_0}{\Delta T} = -1 + 2\sum_{n=1}^{\infty} \lambda_n^{-1}(-1)^{n-1}\cos(\lambda_n x^*)\mathrm{e}^{-\lambda_n^2\tau} \tag{3}$$

in which $x^* = x_1/b$, $\Delta T = T_0 - T_a$, $\lambda_n = \pi(n-1/2)$, $\tau = t\kappa_c/b^2$ is the nondimensional time, and κ_c is the thermal diffusivity of the composite.

2.2. Thermal stress

The temperature field given by Eq. (3) induces normal stresses in both x_2 and x_3 directions in the strip. We assume that the strip undergoes plane strain deformations in the x_1–x_2 plane and is free from constraints at the far ends. The stress in the x_2-direction is

$$\sigma_{22}^{\mathrm{T}}(x^*,\tau) = \frac{E_c\alpha_c\Delta T}{1-\nu_c}\tilde{\sigma}_{22}^{\mathrm{T}}(x^*,\tau) \tag{4a}$$

$$\tilde{\sigma}_{22}^{\mathrm{T}}(x^*,\tau) = -2\sum_{n=1}^{\infty}\lambda_n^{-1}(-1)^{n-1}\cos(\lambda_n x^*)\mathrm{e}^{-\lambda_n^2\tau} + 2\sum_{n=1}^{\infty}\lambda_n^{-2}\mathrm{e}^{-\lambda_n^2\tau} \tag{4b}$$

where E_c is Young's modulus of the composite, ν_c Poisson's ratio and α_c the coefficient of thermal expansion. For spherical metal particles, E_c, ν_c and α_c can be calculated from a micromechanics model [11]:

$$A(\mu_c/\mu_m)^2 + B(\mu_c/\mu_m) + C = 0 \tag{5}$$

$$K_c = K_m + \frac{V_p(K_p - K_m)}{1 + (1 - V_p)\left[(K_p - K_m)/(K_m + 4\mu_m/3)\right]} \tag{6}$$

$$E_c = 9K_c\mu_c/(3K_c + \mu_c) \tag{7}$$

$$\nu_c = E_c/(2\mu_c) - 1 \tag{8}$$

$$\alpha_c = \alpha_p + \frac{\alpha_m - \alpha_p}{(1/K_m - 1/K_p)}\left(\frac{1}{K_c} - \frac{1}{K_m}\right) \tag{9}$$

Here V_p is the volume fraction of metal particles, μ_c is the composite shear modulus, K_c is the bulk modulus, A, B and C are constants depending on μ_m, μ_p, ν_m, ν_p and V_p, and subscripts c, m and p refer to the composite, matrix and particles, respectively. We consider only spherical metal particles, which is a reasonable assumption for most cases. For other shapes of metal particles, the effective properties of the composite and the bridging effect of particles need further investigation. While some progress has been made for the first problem, not much work has been done on the second problem. The thermal stress in the specimen given by Eq. (4) is most severe since a sudden cooling condition has been assumed.

2.3. Integral equation of the thermal crack problem

When the cracked strip is subjected to the thermal shock ΔT, narrow strip damage zones will be developed at the crack tips if the shock ΔT is severe. The damage zones may also be regarded as grown cracks with plastically stretched metal particles bridging the crack surfaces. Because of the symmetry of the problem about the two centroidal axes, only deformations of the material in the first quadrant are analyzed. The boundary conditions for the thermal crack problem are

$$\sigma_{12} = u_1 = 0, \quad x_1 = 0, \quad x_2 \geq 0 \tag{10}$$

$$\sigma_{11} = \sigma_{12} = 0, \quad x_1 = b, \quad x_2 \geq 0 \tag{11}$$

$$\sigma_{12} = 0, \quad 0 \leq x_1 \leq b, \quad x_2 = 0 \tag{12}$$

$$u_2 = 0, \quad 0 \leq x_1 \leq c, \quad x_2 = 0 \tag{13}$$

$$\sigma_{22} = -\sigma_{22}^{T} + H(b - a_0 - x_1)V_p\sigma, \quad c < x_1 \leq b, \quad x_2 = 0 \tag{14}$$

$$\sigma_{\alpha\beta} \longrightarrow 0, \quad 0 \leq x_1 \leq b, \quad x_2 \longrightarrow \infty \tag{15}$$

where $\sigma_{\alpha\beta}(\alpha,\beta = 1,2)$ are stress components, u_α ($\alpha = 1,2$) are displacements, $c = b - a$, $a = a_0 + \Delta a$ is the total crack length, a_0 is the initial crack length, Δa is the crack growth length, $H()$ is the Heaviside step function, σ_{22}^{T} is given by Eq. (4) and σ is the bridging stress of metal particles.

It has been shown that metal particle bridging exhibits a softening behavior [2,4,5] and a linear softening law

$$\sigma = \sigma_0(1 - \delta/\delta_0) \tag{16}$$

may be used [8,9]. Here σ_0 is the maximum bridging stress, δ the crack opening displacement and δ_0 the maximum crack opening at which the bridging is lost.

The longitudinal stress σ_{22} at the crack line ($x_2 = 0$) can be evaluated as [12]

$$\sigma_{22}|_{x_2=0} = \frac{E_c}{2\pi(1-\nu_c^2)}\int_c^b\left[\frac{1}{x'-x_1}+k(x_1,x')\right]\phi(x',\tau)\,\mathrm{d}x' \tag{17}$$

and the singular integral equation of the thermal crack-bridging problem can be deduced as

$$\int_{-1}^{1}\left[\frac{1}{s-r}+K(r,s)\right]\phi(s,\tau)\,\mathrm{d}s = \frac{2\pi(1-\nu_c^2)}{E_c}\left[-\sigma_{22}^{\mathrm{T}}(r,\tau)+H(r-r_0)V_p\sigma_0\left(1-\frac{\delta}{\delta_0}\right)\right], \quad |r|\leq 1 \tag{18}$$

where the unknown function $\phi(r,\tau)$ is given by

$$\phi(x_1,\tau) = \frac{\partial u_2(x_1,0,\tau}{\partial x_1} \tag{19}$$

and $K(r,s)$ is a known kernel singular only at $(r,s) = (-1,-1)$, $r=2(b-x_1)/a-1$ and $r_0=2a_0/a-1$.

Noting the relationship

$$\delta = 2u_2(x_1,0,\tau) = -a\int_r^1\phi(s,\tau)\,\mathrm{d}s \tag{20}$$

Eq. (18) can be written as

$$L[\phi] = -2\pi(1+\nu_c)\alpha_c\Delta T\tilde{\sigma}_{22}^{\mathrm{T}}(r,\tau)+\frac{2\pi(1-\nu_c^2)}{E_c}H(r-r_0)V_p\sigma_0, \quad |r|\leq 1 \tag{21}$$

where the linear integral operator L is

$$L[\phi] = \int_{-1}^{1}\left[\frac{1}{s-r}+K(r,s)\right]\phi(s,\tau)\,\mathrm{d}s - 2\pi V_p H(r-r_0)\left(\frac{a}{b}\right)b^*\int_r^1\phi(s,\tau)\,\mathrm{d}s \tag{22}$$

and

$$b^* = \frac{(1-\nu_c^2)\sigma_0 b}{E_c\delta_0} = \frac{(1-\nu_c^2)b}{2E_cG_f/\sigma_0^2} \tag{23}$$

Here G_f is the fracture energy of the bridging zone:

$$G_f = \int_0^{\delta_0}\sigma\,\mathrm{d}\delta = \frac{1}{2}\sigma_0\delta_0 \tag{24}$$

According to the singular integral equation methods [12,13], Eq. (21) has a solution of the following form if the second integral in Eq. (22) is not considered:

$$\phi(r,\tau) = \psi(r,\tau)/\sqrt{1-r} \tag{25}$$

where $\psi(r,\tau)$ is continuous and bounded on $[-1,1]$. It is shown in [14] that even when the second integral is considered, Eq. (21) still has a solution of the form of Eq. (25).

2.4. Thermal stress intensity factor

The thermal stress intensity factor (TSIF) at the crack tip, $K_{\rm I}$, is given by

$$K_{\rm I} = \frac{E_{\rm c}}{1-\nu_{\rm c}^2}\sqrt{\pi a}\left[-\frac{1}{2}\psi(1,\tau)\right] \tag{26}$$

The solution of Eq. (21) may be expressed as

$$\begin{aligned}\phi(r,\tau) &= (1+\nu_{\rm c})\alpha_{\rm c}\Delta T\phi_1(r,\tau) + \frac{1-\nu_{\rm c}^2}{E_{\rm c}}\sigma_0\phi_2(r,\tau)\\ &= \frac{1}{\sqrt{1-r}}\left[(1+\nu_{\rm c})\alpha_{\rm c}\Delta T\psi_1(r,\tau) + \frac{1-\nu_{\rm c}^2}{E_{\rm c}}\sigma_0\psi_2(r,\tau)\right],\end{aligned} \tag{27}$$

where $\phi_i (i=1,2)$ satisfy

$$L[\phi_1] = -2\pi\tilde{\sigma}_{22}^{\rm T}(r,\tau), \quad |r|\le 1 \tag{28}$$

$$L[\phi_2] = 2\pi V_{\rm p}H(r-r_0), \quad |r|\le 1 \tag{29}$$

The normalized TSIF, K^*, is then given by

$$K^* = \frac{(1-\nu_{\rm c})K_{\rm I}}{E_{\rm c}\alpha_{\rm c}\Delta T\sqrt{\pi b}} = -\frac{1}{2}\sqrt{\frac{a}{b}}\left[\psi_1(1,\tau)+p\psi_2(1,\tau)\right] \tag{30}$$

where

$$p = \sigma_0/(E_{\rm c}\alpha_{\rm c}\Delta T/(1-\nu)) \tag{31}$$

is a dimensionless parameter representing the relative strength of the bridging stress to the thermal shock induced stress.

We have not considered the effect of residual stresses on the stress intensity factor. When the composite is cooled down from the processing temperature to room temperature, microstructural thermal stresses developed in the ceramic matrix may toughen the composite (e.g. see [15,16]). However, in the problem studied here the initial temperature of the composite is much higher than room temperature. Accordingly, the microstructural residual stresses will play a less noticeable role.

2.5. Numerical results and discussion

In the numerical calculations of the TSIF, we consider only the full bridging case, i.e. the crack is fully bridged; the TSIFs for a partially bridged crack in a particular problem may be calculated using the present method. We have neglected the effect of inertia forces in the mechanical problem and have also considered one-dimensional temperature distribution. These assumptions make the problem mathematically tractable without sacrificing too much on the accuracy of the computed stress intensity factor. We note that the thermal stress intensity factor for the dynamically impacted crack is usually 30% higher than that for a static one. The use of one-dimensional temperature distribution is reasonable since the maximum stress intensity factor occurs very shortly after the thermal shock is applied. During the initial stage of the thermal shock, heat mainly flows along the crack with very little, if any, temperature gradient in the direction perpendicular to the crack face.

Fig. 2 shows the normalized TSIF K^* versus the nondimensional time τ for normalized crack length $a/b = 0.01$, 0.17 and 0.30. The TSIFs for monolithic ceramics (without bridging) as well as for MPCMCs with $p = 0.1$, 0.2 and 0.3 are depicted. Here we have neglected the possible bridging of ceramic grains as it is insignificant when compared with the metal particle

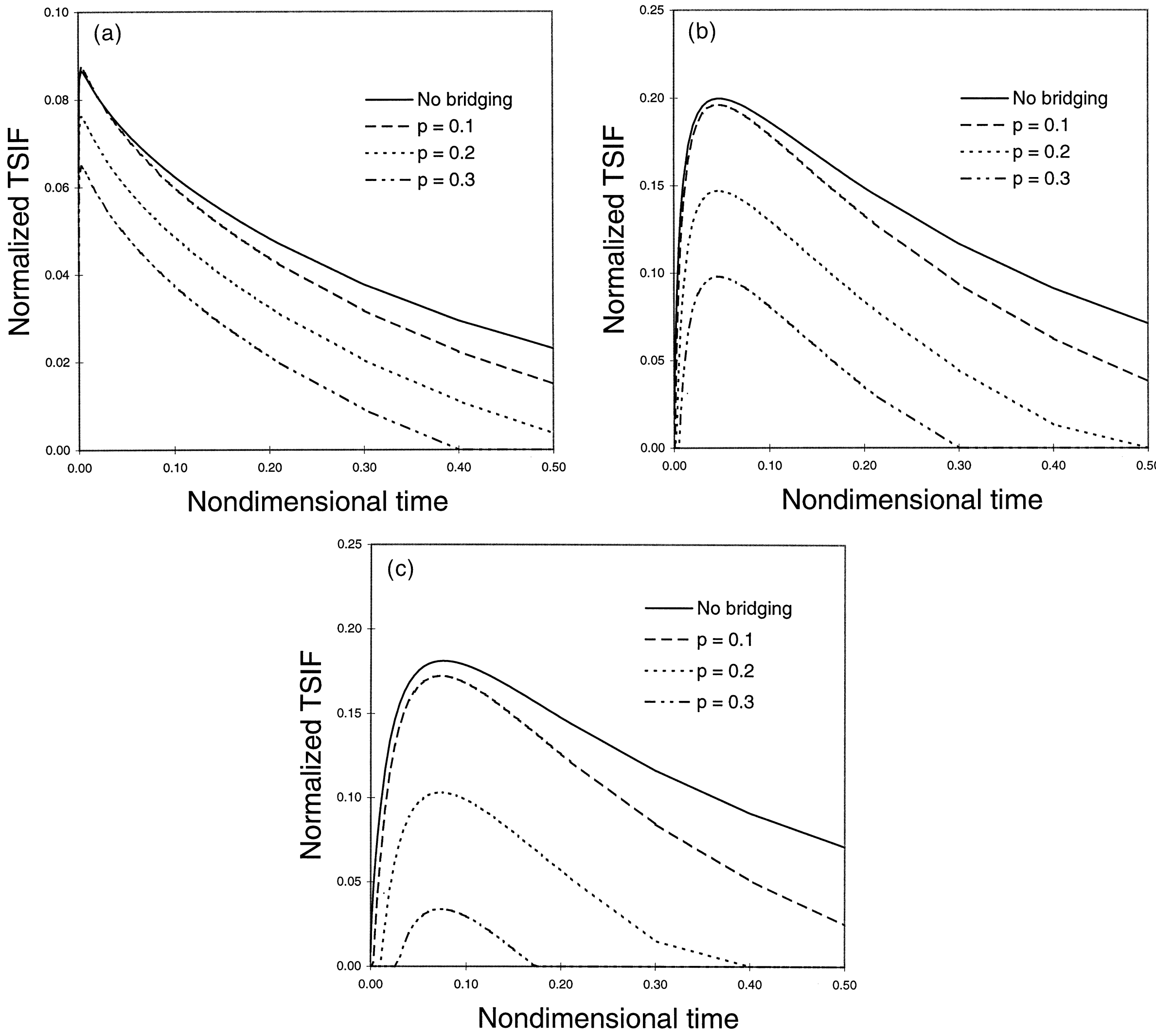

Fig. 2. Normalized thermal stress intensity factor K^* versus nondimensional time τ with and without particle bridging: (a) $a/b = 0.01$; (b) $a/b = 0.17$; and (c) $a/b = 0.30$.

bridging. It is observed from Fig. 2 that for a given normalized crack length a/b, the TSIF increases with time, reaches a peak value at a particular time which increases with the crack length, and then decreases with further increase in time. There exists a critical crack length $l_c(=a_c/b)$ at which the peak TSIF reaches a maximum. The critical value l_c is approximately 0.17 for unbridged cracks and is slightly less than 0.17 when crack bridging is considered. It is clear that thermal crack shielding effect of metal particle bridging is noticeable, i.e. the TSIFs are significantly reduced. For example, the normalized peak TSIF for $a/b=0.17$ is about 0.20 when no bridging is considered. When the particle bridging is considered, the peak TSIF is reduced to about 0.196, 0.147 and 0.098 for $p=0.1$, 0.2 and 0.3, respectively. The bridging effect is more significant for longer cracks. Fig. 3a depicts the normalized peak TSIF versus the nondimensional crack length a/b for monolithic ceramics and Fig. 3b exhibits the results for both monolithic ceramics and MPCMCs for $p=0.1$, 0.2 and 0.3. Note that the TSIFs for ceramics in Figs. 2 and 3b are normalized with respect to the composite properties but in Fig. 3a they are normalized with respect to the matrix material properties. It is interesting to note from Fig. 3 that the TSIFs for longer cracks may be reduced to zero due to metal particle bridging. For example, when $p=0.2$, the TSIF equals zero for cracks with normalized length $a/b>0.5$. This suggests that thermal crack propagation in MPCMCs may be arrested by strong metal particle bridging.

3. Thermal shock damage

When subjected to a thermal shock, an MPCMC with an initial crack of length a_0 will suffer damage, i.e. the crack will grow but will be bridged by the plastically stretched metal particles.

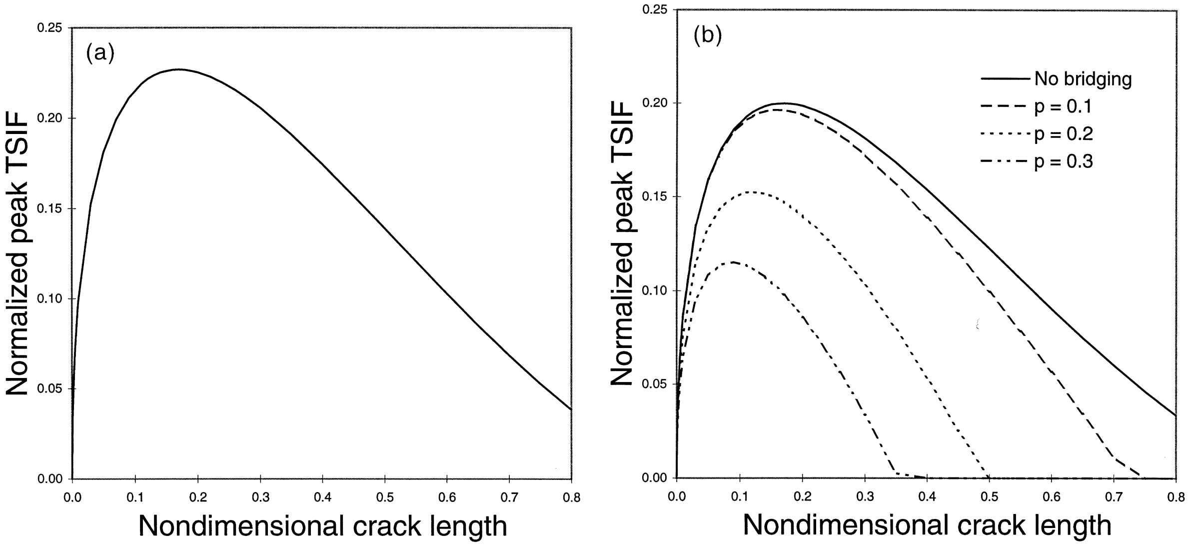

Fig. 3. Normalized peak thermal stress intensity factor versus nondimensional crack length a/b: (a) for monolithic ceramics; and (b) for monolithic ceramics and MPCMCs.

This bridged part of the crack may be considered as a kind of thermal shock damage. Consider the double edge cracked MPCMC specimen subjected to a thermal shock studied in the last section. The thermal shock damage or the crack growth length $\Delta a(=a-a_0)$ may be determined from Eq. (30) by equating TSIF K_I to a critical SIF, K_{cr}

$$\frac{(1-\nu_c)K_{cr}}{E_c\alpha_c\Delta T\sqrt{\pi b}} = -\frac{1}{2}\sqrt{\frac{a_0+\Delta a}{b}}\left[\psi_1(1,\tau_m)+p\psi_2(1,\tau_m)\right] \tag{32}$$

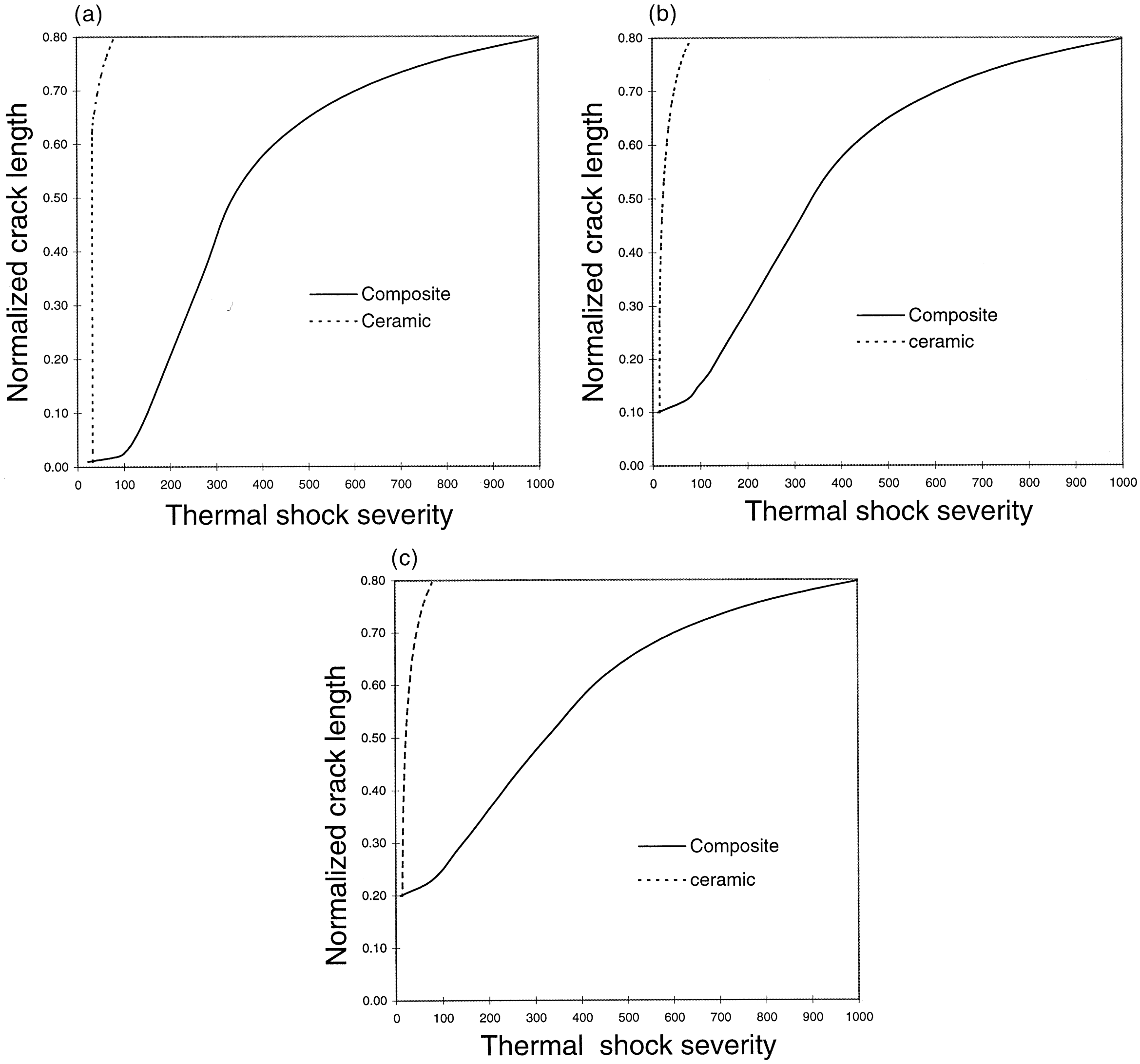

Fig. 4. Normalized crack length a/b versus thermal shock severity ΔT for a Ni/Al_2O_3 composite and monolithic Al_2O_3: (a) $a_0/b=0.01$; (b) $a_0/b=0.1$; and (c) $a_0/b=0.2$.

Table 1
Properties of the component materials of an MPCMC

	Young's modulus (GPA)	Poisson' ratio	Thermal expansion ($10^{-6}K^{-1}$)	Fracture toughness ($MPa\sqrt{m}$)	Yield strength (MPa)	Strain hardening index
Al_2O_3	360	0.20	8	2		
Ni alloy	200	0.33	15	100	800	0.11

where τ_m is the time at which $-[\psi_1(1,\tau_m)+p\psi_2(1,\tau_m)]$ is maximum and K_{cr} is given by

$$K_{cr} = \sqrt{\frac{E_c(1-v_m^2)}{E_m(1-v_c^2)}(1-V_p)}\ K_{mc} \tag{33}$$

with K_{mc} being the matrix fracture toughness.

Fig. 4 shows the normalized total crack length after thermal shock versus the thermal shock severity ΔT for a nickel alloy (Ni) particle reinforced alumina (Al_2O_3) matrix composite for different initial crack lengths. Also shown in the figure is the crack length for the monolithic alumina. The volume fraction of particles is taken as $V_p = 0.3$, the half specimen width b as 10 mm, and three initial crack lengths, i.e. $a_0/b = 0.01$, 0.1 and 0.2 are considered. Table 1 gives material properties of Ni and Al_2O_3. The bridging parameters σ_0 and δ_0 for an average metal particle size of 20 μm are calculated as 1290 MPa and 33 μm, respectively [17]. The calculation is based on the micromechanics model of Mataga [5] and the argument of Bao and Zok [9] to linearize the model. It can be seen from the figure that, although the composite suffers damage,

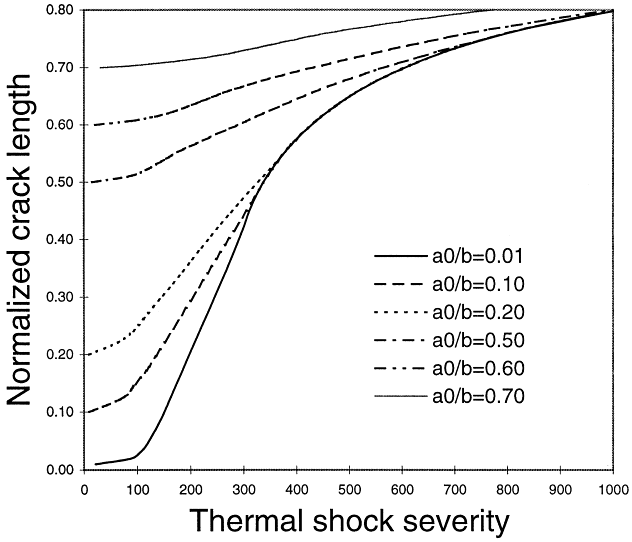

Fig. 5. Normalized crack length a/b versus thermal shock severity ΔT for a Ni/Al_2O_3 composite for various initial crack lengths a_0/b.

the damage behavior is significantly different from that of alumina. For an initial crack length less than about $0.17b$, the crack in alumina will grow unstably under the minimum thermal shock to initiate the crack (for $a_0/b=0.01$, this shock is about 32 K) and under a slightly more severe thermal shock, the crack can easily grow to a normalized length a/b of 0.8. In contrast with alumina, the composite can withstand significantly more severe thermal shocks. For the initial crack lengths considered, a thermal shock of $\Delta T=1000$ K is needed to increase the crack to a length of 0.8. Fig. 5 shows total crack length for the composite after thermal shocks for various initial crack lengths. It is seen that for the initial normalized crack length less than about 0.6, the cracked specimen can always withstand a thermal shock of $\Delta T=1000$ K, i.e. the normalized total crack length a/b of the grown crack is less than 0.8. Even for an initial nondimensional crack length of 0.7, a thermal shock of about $\Delta T=780$ K is needed to increase the crack to a length of 0.8.

4. Conclusions

We have studied thermal crack shielding and thermal shock damage in a double-edge cracked metal-particle-reinforced ceramic matrix composite subjected to sudden cooling at the cracked surfaces. Under severe thermal shocks, the crack will grow but is bridged by the plastically stretched metal particles. It is found that the thermal stress intensity factor is significantly reduced by the metal particle bridging. While the crack growth in thermally shocked monolithic ceramics is unstable, the composite can withstand sufficiently severe thermal shocks without failure. Compared with monolithic ceramics, the composite suffers significantly less thermal shock damage.

References

[1] Krstic VD. On the fracture of brittle-matrix/ductile-particle composites. Phil Mag A 1983;48:695–708.
[2] Evans AG, McMeeking RM. On the toughening of ceramics by strong reinforcements. Acta Metall 1986;34:2435–41.
[3] Budiansky B, Amzigo JC, Evans AG. Small-scale crack bridging and the fracture toughness of particulate-reinforced ceramics. J Mech Phys Solids 1988;36:167–87.
[4] Sigl LS, Mataga PA, Dalgleish BJ, McMeeking RM, Evans AG. On the toughness of brittle materials reinforced with a ductile phase. Acta Metall 1988;36:945–53.
[5] Mataga PA. Deformation of crack-bridging ductile reinforcements in toughened brittle materials. Acta Metall 1989;37:3349–59.
[6] Ashby MF, Blunt FJ, Bannister M. Flow characteristic of highly constrained metal wires. Acta Metall 1989;37:1847–57.
[7] Bannister M, Ashby MF. The deformation and fracture of constrained metal sheets. Acta Metall Mater 1991;39:2575–82.
[8] Bao G, Hui C-Y. Effects of interface debonding on the toughness of ductile-particle reinforced ceramics. Int J Solids Struct 1990;26:631–42.
[9] Bao G, Zok F. On the strength of ductile particle reinforced brittle matrix composites. Acta Metall Mater 1993;41:3515–24.
[10] Carslaw HS, Jaeger JC. Conduction of heat in solids. Oxford: Clarendon Press, 1959.
[11] Christensen RM. Mechanics of composite materials. New York: Wiley, 1979.

[12] Gupta GD, Erdogan F. The problem of edge cracks in an infinite strip. ASME J Appl Mech 1974;41:1001–6.
[13] Muskhelishvili NI. Singular integral equations. Noordhoff: Groningen, 1953.
[14] Jin Z-H, Mai Y-W. Effect of crack bridging on stress intensity factor in thermally shocked ceramics. In: Proceedings of 1st International Symposium on Thermal Stresses and Related Topics. Japan: Hamamatsu, 1995. p. 63–6.
[15] Taya M, Hayashi S, Sobayashi AS. Toughening of a particulate-reinforced ceramic matrix composite by thermal residual stress. J Am Ceramic Soc 1990;73:1382–91.
[16] Li Z, Taya M, Dunn ML. Experimental study of the fracture toughness of a ceramic/ceramic-matrix composite sandwich structure. J Am Ceramic Soc 1995;78:1633–9.
[17] Jin Z-H, Batra RC. Some basic fracture mechanics concepts in functionally graded materials. J Mech Phys Solids 1996;44:1221–35.